

An Acquisition and Distribution System for Situational Awareness

William E. Green, Paul Y. Oh, and Seunghyun Yoon
Drexel University, Philadelphia
Email:[weg22, paul.yu.oh, sy25]@drexel.edu

Abstract

In times of disaster acquiring aerial images is challenging. Runways may be crippled thus denying conventional aircraft in the area from taking off. Also the time required to schedule a satellite fly-by may delay first response efforts. Man backpackable aerial robots can be carried close to the disaster site and flown to capture aerial images. This paper integrates mechatronics, intelligent sensing, and mechanism synthesis in a teleoperable kite-mounted camera. Rapidly deployable, transportable by foot, easy to fly and affordable, our system can quickly acquire, process and distribute aerial images. Image mosaicing, edge detection, 3D reconstruction and geo-referencing resulting from images acquired by our aerial platform are also presented.

1 Introduction

Providing command and control (C2) teams with an additional viewpoint of a disaster scene from the air would supplement their capabilities. Aerial images present useful information that might not be seen from someone on the ground such as the extent of damage, structural integrity of buildings and bridges, and ingress and egress routes to the site and nearby hospitals, respectively. However, in a disaster situation, most of the familiar methods for acquiring aerial images are eliminated. Runways, bridges or helipads can be crippled, destroyed or blocked thus denying access by conventional aircraft or road vehicles. Satellites can provide high resolution images, but reprogramming them for a fly-by introduces unnecessary delays in the mitigation effort. Unmanned Aerial Vehicles (UAVs), like those used in Iraq and Afghanistan for surveillance, usually require a highly trained teleoperator. Finally, remote controlled aircraft demands there be a line-of-sight path between the operator and the vehicle at all times which is not feasible in urban environments. Thus, in disaster mitigation and urban search-and-rescue (USAR)

environments, an aerial image acquisition and distribution system is needed that is rapidly deployable, backpackable, lightweight, and easily controllable.

The future of aerial robots possesses vast capabilities, but current prototypes have several limitations. Lighter-than-air vehicles, like blimps [9], cannot be rapidly deployed. The helium would be backpackable, but inflation times could be long since the buoyancy force of helium is $.064 \text{ lbs/ft}^3$ (1.03 kg/m^3). For an inflation rate of $0.5 \text{ ft}^3/\text{sec}$, it would take over 10 minutes just to lift 20 lbs. Rotary wing aircraft, like helicopters [6] [4] [2], rely on GPS for autonomous navigation and hence, cannot be used in an environment where skyscrapers or adverse weather conditions will occlude line-of-sight. Large fixed-wing aircraft do not possess the ability to hover over the scene like blimps and helicopters to capture lengthy video. Aerial robots need to be more reliable before they can be employed in USAR situations.

Kites are backpackable, rapidly deployable, tethered, which makes them easy to fly, and affordable. Kites can be designed to lift a desired payload such as a 10 lb teleoperated vision system in a minimal wind (e.g. 10 MPH ¹). Such characteristics and public familiarity make kites a very attractive aerial robot platform for aerial image acquisition. This paper presents a Low Elevation Aerial Photography (LEAP) system for acquiring aerial images. LEAP consists of a kite furnished with a teleoperated camera rig and stabilization mechanism, which is fixed to the kite line. Computer vision image processing techniques are then implemented to facilitate the interpretation of raw image data. Finally wireless networking is integrated into our system for rapid distribution to command and control centers. LEAP was awarded the Philadelphia Port of Technology Entrepreneurship in Technology award for its potential in rapid disaster response. LEAP also incorporates a design technique known as

¹At 10 MPH winds, leaves are in motion and lightweight flags extend

partitioning that leverages dynamics when synthesizing a vision system [3] [5]. Section 2 presents the kite's flight dynamics as well as the fundamental theory behind the suspension mechanism. Section 3 describes how the raw images of our system can be processed in order to augment the efforts of command and control teams. Section 4 presents another potential application of LEAP in the environmental engineering field. And Section 5 concludes with our future applications.

2 LEAP Design

In order for a kite to successfully carry a payload, it must be dynamically stable. A number of bottlenecks in the design phase have to be overcome to make this state of dynamic equilibrium possible. First, for a kite to become airborne, wind pressure, rope and tail tensions, and gravity all have to be in dynamic balance. The kite's wingspan, center of pressure, bridle point and tail length must be designed in unison to handle expected wind speeds and lift the desired payload mass. Next, the aerial image acquisition system must be equipped with pan-tilt camera capabilities to acquire images in a specific region of interest. Trying to manipulate a stationary camera's field-of-view by manually controlling the kite's position is irrational. Finally, equipping the kite with such a mechatronic system will introduce torques that can throw the kite's dynamic equilibrium awry. Therefore, a stabilization system is needed to counteract these dynamic instabilities while, at the same time, keeping the camera's attitude constant. We overcame these challenges by systematically integrating the kite flight dynamics, camera mechanics, and a stabilization mechanism into a single system.

2.1 Kite Flight Dynamics

A kite's wingspan can be calculated through dynamic analysis that will enable it to lift a desired payload off the ground. Kites with larger wingspans require thicker and stronger rope and are hard to control. Therefore, trial-and-error approaches to upscale a kite's wingspan are not efficient. Dynamic equilibrium in kites occurs when kite weight w , rope b and tail t tensions and wind force p are in balance as shown in Figure 1. The forces can be extrapolated to meet at a common point, C called the concurrency point. The ground anchor A , bridle point B and tail T are fixed and can be considered as constraints. The center of mass M and center of pressure P are points within the kite's boundaries. Furthermore, for angles of attack α between 15 and 40 degrees relative to the

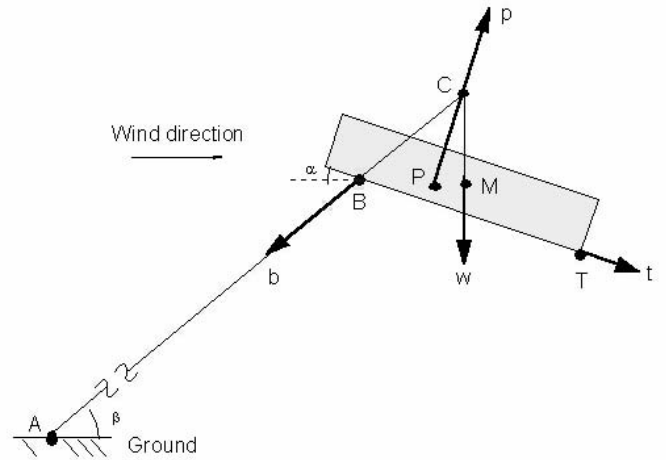


Figure 1: Simple kite model with forces in balance

airstream, the center of pressure location will be virtually stationary and can be assumed to be fixed.

Wind force is proportional to the square of wind speed. Assuming constant kite weight and an unstretchable rope, changes in wind speed will result in a force imbalance thus prompting kite and/or tail movement. For most kites, the location of the bridle point B is often a small distance away from the kite's sail and hence movement about B will be small. With tail force typically being small, the only remaining movement possible is about A . Aerodynamically, to compensate for force increase arising from higher wind speed, the kite must decrease its angle of attack. This is a counter-clockwise arching in Figure 1 and is the marvel of kite flight dynamics; in this non-linear dynamic balancing act, the kite flies into new states of stability.

Analyzing the forces acting on the kite allows the derivation of a kite's wing span needed to successfully airlift a payload in an expected wind speed. The underlying physics can be appreciated by assuming a kite sail that is square with sidelength L . The result is a wind force acting on an effective area of $A = L^2$. Furthermore, this wind force acting at the center of pressure P (see Figure 1) is proportional to the kite's effective area and the square of wind speed V^2 . The balance of forces p , w and b discussed above dictates that $w \approx AV^2$ or

$$V^2 \approx \frac{w}{A} \quad (1)$$

That is, wind speed squared is proportional to kite/payload weight divided by the kite sail area. Independent of wind speed is buoyancy which dictates

a constant mass ratio μ (mass of air displaced versus mass of kite). Kite mass is proportional to its weight w . The displaced air mass, being a volume, must be proportional to another volume, namely L^3 . This yields

$$\mu \approx \frac{L^3}{w} \quad (2)$$

In other words with a constant mass ratio, upscaling a stable kite to a sidelength $L' = XL$ where $X > 1$ will result in a new effective area $A' = X^2A$ and from Equation 2, the new kite weight is $w' = X^3w$. From Equation 1, the new wind speed required to be airborne is $V' = VX^{1/2}$. Such upscaling results in weight growing with volume, loss of stability at higher wind speeds and more wind being needed to remain airborne.

Alternatively, changing the mass ratio (e.g. using a heavier kite) can increase stability. For a specific wind speed V , an upscaling with $L' = XL$ where $X > 1$ will increase effective area $A' = X^2A$ and from Equation 1 results in $\frac{w'}{A'} = \frac{w}{A}$. Thus kite weight grows with area and yields $\mu' = X\mu$.

The net effect is that given a kite that flies stably at a specific wind speed or defined mass ratio, the necessary changes in wing span can be calculated.

2.2 Camera Rig Mechatronics

A 2.4 GHz camera is mounted on a mechatronic rig (see Figure 2) which is suspended from the kite line using a stabilization mechanism. The rig has 2 radio-controlled (r/c) servos which allow the user to pan and tilt the camera to capture a desired region. The camera's video is fed into a wireless transmitter which sends the signal down to a ground-based receiver. The receiver is linked to a handheld portable video camera with an LCD screen so that camera's field-of-view can be "seen" live from the ground while also recording the footage.

After capturing this aerial video, time is the biggest constraint. In a dynamic environment like a disaster, a lot can change over the time it takes to transport the video back to the nearest command and control center, process and then distribute the images. However, the video can be digitized out in the field by interfacing the camera's IEEE1394 firewire capabilities with a laptop computer. Equipped with an 802.11b wireless networking card, the base stations in the field permit the digitized video to be streamed over the web in real-time. Therefore, any personnel with internet access can also monitor the camera's field-of-view.

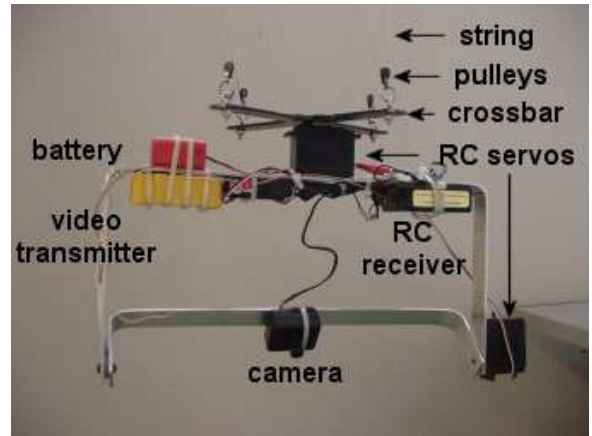


Figure 2: Mechatronic camera rig designed with RC servos, 1/4 mile range 4 mm lens focal length, and video transmitter. Pan and tilt range are both $\pm 30^\circ$

2.3 Picavet

Mounting the camera rig directly to the kite line is feasible, but not efficient. Winds will force the rig into a swaying motion. This will introduce a torque that will destabilize the kite and eventually cause it to crash. Furthermore, positioning the camera via the R/C servos to capture a particular area will prove to be extremely difficult without any camera stability. A suspension mechanism based on an elliptical pendulum, known as the Picavet (pronounced "peekaway"), can be integrated to keep the camera rig's attitude constant despite changes in the kite's orientation. The net effect is that the camera's image plane can be stabilized and therefore will be easily controllable.

The Picavet suspension system is comprised of a crossbar with pulleys at each of the four ends, two brackets, each with a single pulley, which are fixed to the kite line, one continuous rope which loops through all 6 pulleys, and a ring which constrains the two innermost lines as they cross. So as the kite increases or decreases its altitude, the rope glides effortlessly through the pulleys keeping the camera rig in a constant position. Similarly, if the camera rig was initially in a skewed position with the crossbar being at some angle to the ground, it would sustain this position throughout flight.

A simulation was used to show the Picavet's response to a change in the kite's altitude (see Figure 3). The photo on the left reveals the position of the rig at the kite's initial attitude with the camera's image plane being parallel to the ground. The photo in the mid-

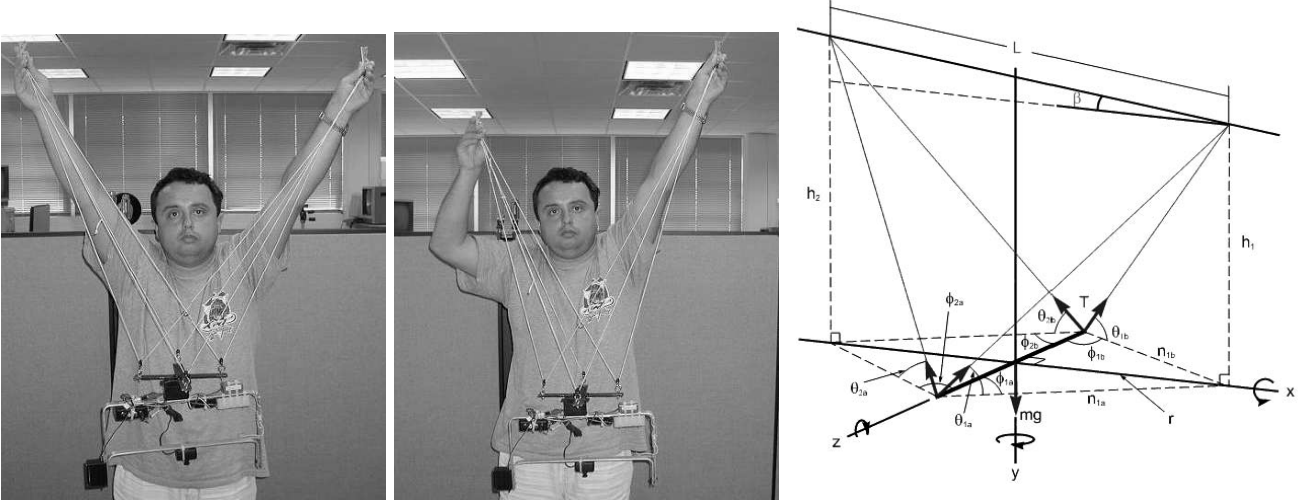


Figure 3: Left: Picavet initial attitude. Middle: Attitude is unchanged despite pendulum sway. Right: Picavet free body diagram

dle shows the rig undisturbed despite a change in the kite's orientation.

The Picavet's system dynamics were analyzed in three-dimensional space to prove the stability phenomenon. A free body force diagram of a simplified version of the Picavet is shown in Figure 3 (right). The tension forces are homogeneous because a single rope is used to loop through the pulleys. The z-axis is aligned with the axis of the bar while the x and y axes pass through the midpoint of the bar and are perpendicular to it. This results in ϕ_{1a} , ϕ_{1b} , θ_{1a} and θ_{1b} being less than 90 degrees. Furthermore

$$\tan \phi_{1a} = \tan \phi_{1b} = \frac{r}{l_{\text{bar}}/2} \quad (3)$$

And because ϕ_{1a} and ϕ_{1b} have to be less than 90 degrees, $\phi_{1a} = \phi_{1b}$. These two triangles also share a common side, r , which indicates that $n_{1a} = n_{1b}$. We also have

$$\tan \theta_{1a} = \frac{h_1}{n_{1a}} \quad \text{and} \quad \tan \theta_{1b} = \frac{h_1}{n_{1b}} \quad (4)$$

Hence $\tan \theta_{1a} = \tan \theta_{1b}$ and since θ_{1a} and θ_{1b} are both less than 90 degrees, we have $\theta_{1a} = \theta_{1b}$. Similarly

$$\phi_{2a} = \phi_{2b} \quad (5)$$

$$\theta_{2a} = \theta_{2b} \quad (6)$$

The z-axis is assumed to go through the center of the bar and thus, the moment will be zero, $\Sigma M_z = 0$. Furthermore, the rotation about the y-axis will not disturb the camera's image plane relative to the ground

and will be disregarded. Therefore, proving there are no external moments about the bar's center of mass in the x-direction, $\Sigma M_x = 0$, will show that the camera rig's attitude will remain constant. We will assume counterclockwise to be the positive direction and taking the sum of the moments, we have

$$\begin{aligned} \Sigma M_x = & -\frac{1}{2}Tl_{\text{bar}} \sin \theta_{1a} - \frac{1}{2}Tl_{\text{bar}} \sin \theta_{2a} \\ & + \frac{1}{2}Tl_{\text{bar}} \sin \theta_{1b} + \frac{1}{2}Tl_{\text{bar}} \sin \theta_{2b} \end{aligned} \quad (7)$$

3 Disaster Mitigation

Raw aerial data can be difficult to interpret to the unfamiliar eye (e.g. unmarked roads and buildings). Therefore, image processing techniques must be employed to assist in the comprehension of raw images. Substituting current methods of C2 communication with this well-constructed imagery would facilitate communication efforts in emergency and time-critical situations.

3.1 Image Processing

A stationary camera typically has a field-of-view of only 50 degrees and hence, apx. two city blocks can be captured in an image taken at 1000 feet (approximately 70 building stories). In order to provide C2 teams with views of the surrounding areas and the capability of mapping out ingress and egress routes, processing techniques such as image mosaicing, 3D reconstruction, and text overlay will be invoked. Image mosaicing involves stitching several images together to

yield a single larger image that gives a panoramic view of a scene (see Figure 4). The method of mosaicing [7] identifies and relates common points among two or more images. Any two common points are related to each other by a translation and a rotation. Four common points, two in each image, are needed to generate the transformation matrix, M . Once, the transformation matrix is known, the points in the original images, u , can be mapped algorithmically to the mosaiced image, u^1 , by the relation $u^1 = Mu$.

Once the raw data is acquired, command and control teams are limited by whatever details are visible in the two-dimensional image. Beyond zooming and cropping, the viewer cannot interact with the image and hence, little information can be gathered. 3D Reconstruction (3DR) is the computer vision technique that creates a graphical model from 2D images [8]. Within a VRML-enabled web browser², the incident commander can rotate, pan and zoom the 3D models to navigate through streets and around buildings to gather information and search for victims. Figure 4 (middle) shows the 3D reconstructed model of the image still using a commercial version of Facade [1] called Canoma.

3.2 Real-Time Communication

Although such image processing techniques facilitate the interpretation of raw data for C2 teams, it is extremely time intensive. Acquiring, processing and distributing the images are independent procedures and thus, delay C2 capabilities. These three stages had to be integrated together and performed at once to be most beneficial. We envisioned first-responders and other C2 personnel equipped with handheld devices like Palm Pilots in order to receive visual commands such as ingress and egress routes to victims and hospitals respectively, during a disaster situation.

Real-time image processing software was developed to be run at a command and control base station (See Figure 4). The images acquired by our *LEAP* system can be wirelessly transmitted to the station where they will be processed and uploaded to a web server in real-time. In order for these images to be downloaded, additional PDA software with a "user-friendly" front end was developed. The net effect was a real-time wireless imagery acquisition and distribution system.

²<http://prism.mem.drexel.edu/projects/kite/index.html> hosts the VRML model where one can virtually fly through an urban area near West Philadelphia

4 Valley Creek Watersheds

A watershed is the area of land from which rainfall drains into a stream or other water body. In order to locate watersheds and assess their change over time, aerial photographs are taken every 5 years by the local government. However, the photographs are taken from altitudes of over 3000 feet with a low-resolution black-and-white camera (See Figure 5). This makes the photographs virtually useless to environmental research groups. Instead, we believe our developed kite and teleoperated vision system will provide research teams with the detail needed to make accurate assessments. Streams are typically lined with trees and grass and therefore, might be hard to identify during the flourishing seasons. However, edge detection and image mosaicing can be used to filter the image (while still preserving the outline of the stream) and create a single image that captures the stream in its entirety respectively.

5 Conclusion

This paper presented a Low Elevation Aerial Photography (*LEAP*) system to overcome many obstacles prevalent in time-critical dynamic environments such as disaster situations. Runways may be crippled preventing conventional aircraft from taking off; roads could be damaged eliminating access to ingress and egress routes; and radio-controlled or robotic aerial vehicles like blimps, helicopters or fixed-wing aircraft require skilled teleoperators. *LEAP* is an easy-to-fly, man-backpackable, quickly deployable and affordable kite and teleoperated vision system for acquiring aerial images. Processing techniques such as image mosaicing, 3D reconstruction and text overlay were implemented to facilitate the interpretation of the raw data captured by *LEAP*. The use of this well-constructed imagery can eliminate the ambiguities sometimes present when relying on voice-based communications. Ingress/egress routes can be superimposed over images acquired by *LEAP* and distributed by our real-time image processing software to command and control teams equipped with Palm Pilots or other handheld devices. The net effect is an efficient aerial image acquisition and distribution system through the integration of mechatronics, intelligent sensing, mechanism synthesis and computer vision.

References

- [1] Debevec, P., Taylor, C.J., Malik, J., "Modeling and Rendering Architecture from Photographs: A Hybrid

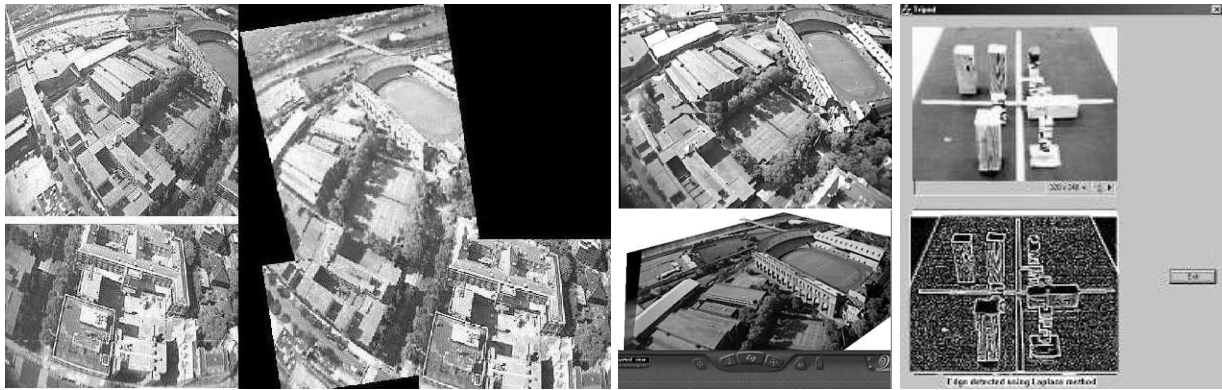


Figure 4: Image mosaic created from disparate aerial images of area near 30th Street Station (left). 3D reconstructed model (bottom) of aerial image (top). Real-time image processing software to be run in C2 base station (far right).



Figure 5: An aerial photograph of valley creek at apx. 3000 ft (left) is hard to interpret compared to some initial images taken by LEAP (middle and right).

- Geometry-and-Image-based Approach”, *Proc. SIGGRAPH 96 Computer Graphics Proc.*, Annual Conference Series, New Orleans, pp. 11-20, Aug. 1996.
- [2] Hamel, T.; Mahony, R., Chriette, A., “Visual Servo Trajectory Tracking for a Four Rotor VTOL Aerial Vehicle”, *IEEE International Conference on Robotics and Automation (ICRA)*, Washington, D.C., pp. 2781-2786, 2002.
 - [3] Oh, P.Y., Allen, P.K., “Visual Servoing by Partitioning Degrees of Freedom,” *IEEE Transactions on Robotics and Automation*, V17, N1, pp. 1-17, February 2001
 - [4] Sharp, C.S., Shakernia, O., Sastry, S.S., “A Vision System For Landing an Unmanned Aerial Vehicle *IEEE International Conference on Robotics and Automation (ICRA)*, Seoul, Korea, pp. 1720-1727, 2001.
 - [5] Stanciu, R., Oh, P.Y., “Designing Visually Servoed Tracking to Augment Camera Teleoperators”, *IEEE Conference on Intelligent Robotics and Systems (IROS)*, Lausanne Switzerland, Oct. 2002.
 - [6] Saripalli, S., Montgomery, J.F., Sukhatme, G.S., “Vision-based Autonomous Landing of an Unmanned Aerial Vehicle”, *IEEE International Conference on Robotics and Automation (ICRA)*, Washington, D.C., pp. 2799-2804, 2002.
 - [7] Szeliski, R., “Video Mosaics for Virtual Environments”, *IEEE Computer Graphics and Applications*, Vol. 16, No. 2, pp. 22-30, 1996
 - [8] Taylor, C., Kriegman, D., “Structure and Motion From Line Segments in Multiple Images,” *IEEE Trans Pattern Analysis and Machine Intelligence (PAMI)*, V17 N11 pp. 1021-1032, 1995
 - [9] Zhang, H., Ostrowski, J.P., “Visual Servoing With Dynamics: Control of an Unmanned Blimp”, *IEEE International Conference on Robotics and Automation (ICRA)*, Detroit, pp. 618-623, 1999.